Josephson junctions defined by a nanoplough

B. Irmer,[a)] R. H. Blick, F. Simmel, W. Gödel, H. Lorenz, and J. P. Kotthaus
Center for NanoScience and Sektion Physik, Ludwig-Maximilians-Universität München, 80539 München, Germany

We define superconducting constrictions by ploughing a deposited Aluminum film with a scanning probe microscope. The microscope tip is modified by electron-beam deposition to form a nanoplough of diamond-like hardness which allows the definition of highly transparent Josephson junctions. Additionally, a dc superconducting quantum interference device is fabricated in order to verify the junction's behavior. The devices are easily integrated in mesoscopic devices as local radiation sources and can be used as tunable on-chip millimeter-wave sources. © *1998 American Institute of Physics.* [S0003-6951(98)04140-0]

Ploughing is a well-known technique used since the earliest days of agricultural cultivation.[1] By scaling this tool down in size to a few nanometers and combining it with conventional scanning probe techniques, we facilitate ploughing of thin-film superconductors on semiconductor samples with nanometer resolution. In the more common atomic force microscope (AFM) scratching techniques, the tip is scanned under strong loading forces to remove the substrate[2] or resist.[3] Our technique utilizes the principle of ploughing in the same way as the traditional tool: material is removed from the substrate in a well-defined way, leaving behind deep trenches with the characteristic shape of the plough used. The advantages of applying a nanoplough for lithography are obviously the precision of alignment, the nondamaging definition process compared to electron- or ion-beam structuring techniques, and the absence of additional processing steps, such as etching the substrate. Furthermore, our technique allows the fabrication of highly transparent superconducting microbridges with constant (Dayem bridge) or variable thickness with almost ideal Josephson behavior.[4,5]

The main advantage of transparent junctions is the lower resistance, and hence, the higher critical current densities j_c of typically 10^6 A/cm^2 in comparison to $j_c \approx 10^2$ A/cm^2 for tunneling junctions.[6] This is expected to result in a dramatically enhanced microwave emission from these junctions. Recent theoretical work points out the importance of these junctions regarding multiple Andreev reflection[7] and makes them of special interest in the field of mesoscopic physics. One aspect in this field is the possibility of creating highly transparent Josephson junctions, which radiate in the microwave range and which can be placed directly by the sample. Here, we use the nanoplough to generate on-chip Josephson junctions suited as microwave sources. We focus on the ploughing technique and on the Josephson characteristics of the constrictions formed. Finally, we describe the superconduction junctions' characteristics and show data on single junctions and from the superconducting quantum interference device (SQUID) taken at dilution refrigerator temperatures.

We define our devices in aluminum thin films with thickness around 100 nm, which are thermally evaporated onto semi-insulating GaAs substrates. In order to achieve reasonable superconducting properties, the background pressure is kept low, typically, at $p \leq 10^{-7}$ mbar with high evaporation rates ≈ 100 Å/s. 2 μm wide wires and loops with 10 μm inner radius are predefined with optical lithography.

A crucial point for nanoploughing is the appropriate plough: common scanning probe microscope tips are either robust but too blunt to form small trenches (Si$_3$N$_4$ or hard coated tips) or too brittle for this purpose (single-crystal Si). We employ *electron-beam deposition* (EBD) to grow material onto the end of common Si tips by focusing the beam of a scanning electron microscope. The highly energetic electrons interact with additionally introduced organic gases and form an organic compound, known as high dense carbon.[8] This material shows a hardness comparable to that of diamond[9] in combination with being nonbrittle.[10]

For the nanoplough 500 nm long and 50 nm wide, needle-like tips are grown under a nonzero angle with respect to the axis of the pyramidal Si tip. Special care has to be taken to ensure a robust interface between the EBD tip and the silicon pyramid. When dragged through material with a lateral force F_l, this angle causes an additional vertical force component F_v, which ensures the plough to be pushed downwards, cutting its way through the material (see the upper inset in Fig. 1).

Imaging and positioning is done in standard AFM mode. In the ploughing mode, the tip is displaced by nominally 1 μm towards the surface, resulting in a loading force $F_\perp \approx 40$ μN, sufficient to completely remove the metal layer. Weak scratches in the GaAs substrate can be seen, thus avoiding a short circuit of the junction by a thin metal layer. To define the Josephson constriction of width w, the tip is withdrawn from the surface, displaced by length w, and driven into the metal layer again. The length L of the Josephson contact is defined by the width of the trench, which again is given by the tip diameter. To date, we were able to cut 300 nm thick Al films with a minimum linewidth of 50 nm, yielding an aspect ratio of 1:6. Figure 1 depicts the SQUID geometry used with the optically predefined constrictions.

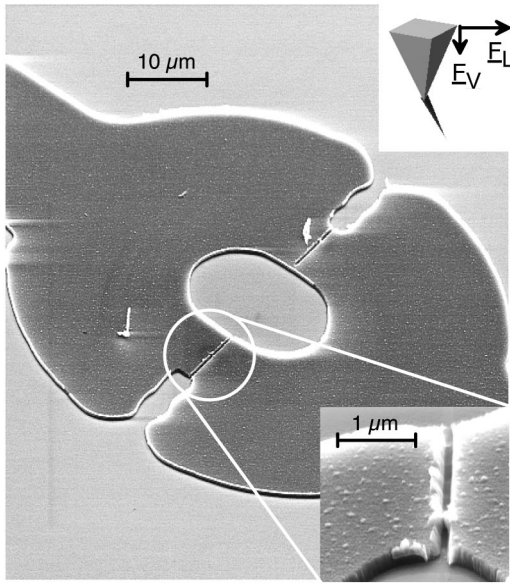[a)]Electronic mail: bernd.irmer@physik.uni-muenchen.de

FIG. 1. Scanning electron microscope micrograph of a double junction SQUID: The junctions are generated in the Al film at the optically predefined constrictions. The lower-right inset shows a magnification of one of the junctions—it can be clearly seen that all the material is removed. The upper inset shows a schematic representation of the nanoplough: the EBD tip is deposited with an angle on a common AFM tip, causing a vertical force F_v when dragged through the material.

The ploughed lines can be seen perpendicular to the direction of the current flow. The upper-right inset depicts a schematic drawing of the nanoplough and the force diagram as mentioned above. A typical junction is shown in the lower right inset with a width and length of 100×100 nm^2. The material removed is pushed up onto the edges of the trench.

In Fig. 2 the characteristic IV trace of a single Al junction is shown, taken at a temperature of 35 mK. Here, a current is fed through the junction and the voltage drop across it is monitored (see the inset with the circuit diagram). The dc-Josephson current can be clearly seen. For currents larger than the critical current I_c, a finite voltage drops across the junction, defined by its normal resistance $R_n = 0.57 \Omega$. The curve agrees well with the theoretical description for a nontunneling, Dayem-bridge-like superconducting weak link described by Likharev.[6] The final devices show a
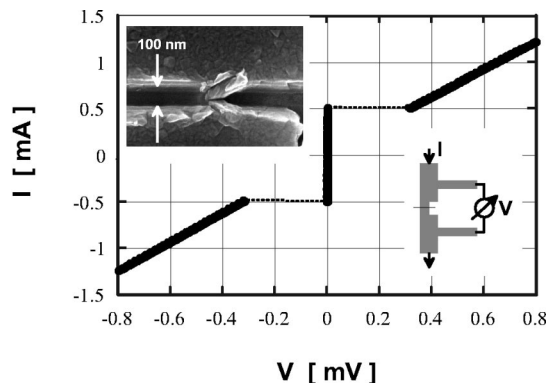

FIG. 2. Characteristic IV trace of a single Josephson junction at $T_{bath} = 35$ mK. The thickness of the Al film is 100 nm, yielding a maximum critical current density of $j_c = 5.1 \times 10^6$ A/cm^2. The upper inset shows the junction with a typical width of 100 nm, the lower inset gives a simplified circuit diagram.
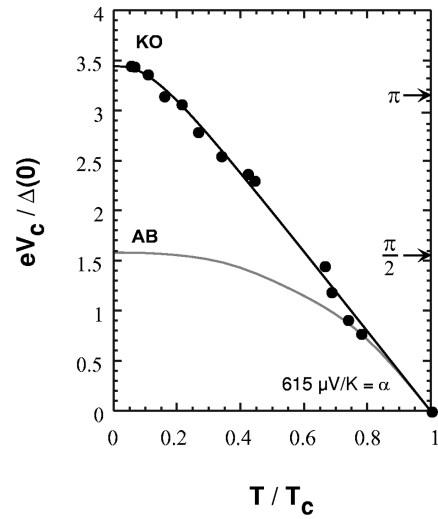

FIG. 3. Temperature dependence of the normalized critical current: black dots indicate our measurements compared to the theory for a tunneling junction (Ambegaokar and Baratoff: AB) and for a clean weak link with $L \ll l, \xi$ (Kulik and Omelyanchuk: KO). KO theory predicts a critical current of π for $T/T_c = 0$. The universal slope $\alpha = \partial(R_N I_c)/\partial T$ for $T \rightarrow T_c$ implies $\alpha = 615$ μV/K in good agreement with the theoretical value $\alpha = 635$ μV/K. This device shows a critical temperature $T_c = 950$ mK.

critical temperature of $T_c = 950$ mK, compared to $T_c \approx 1.2$ K for bulk Al. From its critical temperature we calculate the BCS gap $\Delta_{Al}(T \rightarrow 0) = 3.37/2k_B T_c = 138$ μeV.[11] The associated clean limit coherence length $\xi_{Al} = 0.18 \hbar v_F/(k_B T_c)$ is then $\xi_{Al} = 2.9$ μm,[12] using the bulk Fermi velocity of $v_F = 2.03 \times 10^6$ m/s. This should be compared to the effective length L_{eff} of the Josephson constriction, which is somewhat larger than the 100 nm geometric length, but still an order of magnitude smaller than ξ, which makes our junction extremely transparent.[6,7]

To be applicable as a radiation source, the critical current, and therefore, the amplitude of the ac current has to be large and the capacitance has to be small so as not to shunt the junction. Both requirements are met by transparent junctions. The energy-gap frequency defines an upper limit for the emission at $\nu_c = 2\Delta/h \approx 400$ GHz. The critical current density (Fig. 2) is estimated to be $j_c = I_c/ld = 5.1 \times 10^6$ A/cm^2. From the temperature dependence of the critical voltage $V_c = I_c R_n$ (Fig. 3) we reproduce the universal, material independent slope $\alpha = \partial(R_N \cdot I_c)/\partial T = 2\pi k_B/7\zeta(3)e$ for $T \rightarrow T_c$. This also identifies the conduction mechanism inside the junction: the Kulik–Omelyanchuk theory (KO: straight line)[13] for the case of a clean weak link, i.e. $\xi, l \gg L_{eff}$, where l is the mean-free path of electrons, fits very well to our data. A tunneling junction in comparison would deliver much lower critical currents (Ambegaokar–Baratoff: AB).[14]

To verify the magnetic response of our junctions, we fabricated the two-junction SQUID shown in Fig. 1, where the maximum critical current oscillates as $I_{max} = 2I_c|\cos(\pi\phi/\phi_0)|$, with ϕ being the trapped flux and ϕ_0 being the flux quanta. The enclosed area A is $(10 \mu m)^2 \pi$, yielding an oscillation in magnetic flux density of $\delta B = \phi_0/A = (h/2e)/A = 6.4$ μT, which is well below the critical field of $B_c = 15$ mT. In Fig. 4 the critical current, taken from about 100 IV traces, is plotted against the applied ex-
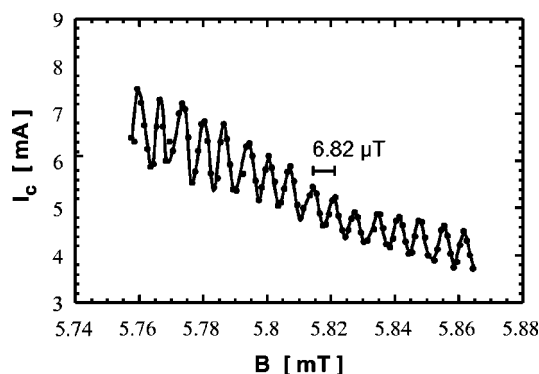
FIG. 4. SQUID data showing the magnetic-field dependence of the critical current density. The line is a guide to the eye. The measured period of 6.82 μT is in excellent agreement with $\delta B = \phi_0/A = (h/2e)/A = 6.4$ μT.

ternal magnetic field. The SQUID junctions had a width and length of 200×100 nm^2, therefore carrying even higher critical currents than the single junction above. The measured period of 6.82 μT is in excellent agreement with the predicted $\delta B = 6.4$ μT. The successful operation of the SQUID assures functioning of the Josephson junctions. Our current device is expected to generate radiation with frequencies around several 100 GHz, limited only by the capacitance of the junction and the pair breaking energy.

In summary, we have fabricated small weak links in Al thin films using a nanoplough technique. These junctions show high critical current densities, low capacitive coupling, and high intrinsic frequencies. The junctions are ideally suited as tunable microwave on-chip devices. A straightforward application of this technique is the integration into mesoscopic systems, e.g., quantum dots or nanotubes.

[1] To the best of our knowledge ploughs are depicted for the first time on small clay plaques found at Uruk IV in Iraq, dated around 3200 BC.

[2] C. Hahn, T. Matsuyama, U. Merkt, and R. Wiesendanger, Appl. Phys. A: Mater. Sci. Process. **62A**, 289 (1996).

[3] L. L. Sohn and R. L. Willett, Appl. Phys. Lett. **67**, 1552 (1995); T. A. Jung, A. Moser, H. J. Hug, D. Brodbeck, R. Hofer, H. R. Hidber, and U. D. Schwarz, Ultramicroscopy **42**, 1446 (1992).

[4] J. E. Mooij, C. A. Gorter, and J. E. Noordam, Rev. Phys. Appl. **9**, 173 (1974).

[5] T. M. Klapwjik and T. B. Veenstra, Phys. Lett. **47A**, 351 (1974).

[6] K. K. Likharev, Rev. Mod. Phys. **51**, 101 (1979).

[7] A. V. Zaitsev and D. V. Averin, Phys. Rev. Lett. **80**, 3602 (1998).

[8] M. Wendel, B. Irmer, J. Cortes, J. P. Kotthaus, A. Lorke, and E. Williams, Superlattices Microstruct. **20**, 349 (1996).

[9] H. Lorenz, J. Lechner, and I. Eisele, Surf. Coat. Technol. **47**, 746 (1991); C. A. Davis, G. A. J. Amaratunga, and K. M. Knowles, Phys. Rev. Lett. **80**, 3280 (1998).

[10] NanoTools GmbH, Schillerstr. 6, 85101 Lenting/Germany (info@nanotools.com).

[11] BCS theory predicts a numerical factor of 3.52, whereas experiments on bulk Al give 3.37 ± 0.1 [see, for example, *Handbook of Chemistry and Physics*, 72nd ed. (CRC, Boston, MA, 1992)].

[12] M. Tinkham, in *Introduction to Superconductivity*, 2nd ed., edited by B. Bredford and M. Gardner (Robert E. Krieger, New York, 1996), pp. 93–94.

[13] I. O. Kulik and A. N. Omelyanchuk, Sov. J. Low Temp. Phys. **3**, 945 (1977).

[14] V. Ambegaokar and A. Baratoff, Phys. Rev. Lett. **10**, 86 (1963).